Tetragonal polymerized phase of C_{60}

V. A. Davydov, L. S. Kashevarova, and A. V. Rakhmanina
Institute for High Pressure Physics of the Russian Academy of Sciences, 142092, Troitsk, Moscow Region, Russian Federation

V. Agafonov, H. Allouchi, and R. Ceolin
Laboratoire de Chimie Physique, Faculté de Pharmacie de l'Université de Tours, 31 Avenue Monge, 37200 Tours, France

A. V. Dzyabchenko
Karpov Institute of Physical Chemistry, ul. Obukha, 10, Moscow 107120, Russian Federation

V. M. Senyavin
Chemistry Department, Moscow State University, Moscow 119899, Russian Federation

H. Szwarc
Laboratoire de Chimie Physique des Matériaux Amorphes, URA 1104, CNRS, Bâtiment 490, Université Paris XI, 91405, Orsay, France
(Received 18 May 1998)

Experimental evidence of the existence of the polymerized tetragonal (*T*) phase of C_{60} as a stable high-pressure one is presented. Using different *p,T* paths of high-pressure–high-temperature treatment, phase *T* was obtained as a product of phase conversions of a monomeric fcc and two polymerized phases of C_{60} (including a rhombohedral one) at 2.2 GPa and 873 K. The dramatic differences in the rates of phase-*T* formation from monomeric and polymerized states of the system testified to the difference in the mechanisms of phase-*T* formation. The x-ray-diffraction pattern, IR, and Raman spectra of the almost pure phase *T* are presented. [S0163-1829(98)02441-2]

Studies of solid-state transformations of C_{60} fullerene revealed some problems related to the identification of carbon states arising at high-pressure–high-temperature treatment (HPHTT). In particular, the difficulties of the pure tetragonal (*T*) polymerized phase synthesis were already noted in the earlier studies,[1,2] which were devoted to the investigation of pressure-induced polymerization and the identification of the polymerized phases of C_{60}. This phase has been observed only in mixtures with either the orthorhombic (*O*) or rhombohedral (*R*) polymerized phases of C_{60}.[2–9] This fact has become the basis of the assumption that the *T* phase has no corresponding stability region in the *p,T* diagram and therefore it cannot be obtained in the pure form. According to one hypothesis, the *T* structure might not, in fact, exist as a stable structure but may be simulated by locally intertwined *O* lattices.[8] Another hypothesis suggests that the *T* structure is simulated by a large number of random crosslinks in a basically *R* lattice.[9,10] Thus, in both cases it was assumed that, unlike the *O* and *R* phases, phase *T* is not a real stable high-pressure phase of the C_{60} system, but rather some growth fault of the *O* or *R* phase.

On the other hand, theoretical calculations show that tetragonal polymerized C_{60} layers are of the same order of stability as rhombohedral ones.[11] Furthermore, our potential-energy calculations with a nonbonded potential resulted in crystal packing of tetragonal layers of $P4_2/mmc$ symmetry with a deep minimum.[12] That is, the results of theoretical investigations did not deny the idea of *T* phase stability at some *p,T* conditions (we apply here the term ''stability'' assuming a relation with respect to other polymerized C_{60} phases while all of them are metastable in the sense of the general carbon *p,T* diagram).

Though a possibility of the direct $R \rightarrow T$ phase transition in the process of isothermal unloading the system from 6.0 to 2.5 GPa at 873 K was already pointed out in our preliminary study,[13] the aim of the present work is to obtain firm experimental evidence supporting the existence of phase *T* as an individual substance. It was assumed that the synthesis of the same phase via different intermediate states is quite a good demonstration of phase-*T* stability.

Three different paths (shown by arrows 1, 2, and 3 in Fig. 1) were chosen to reach the point of 2.2 GPa and 873 K accepted as phase-*T* synthesis conditions according to the *p,T* diagram published earlier.[4]

In the presented diagram fragment of Fig. 1, region *M* corresponds to the monomeric molecular-crystalline state. Region *Mp* corresponds to the different (in the present study, *T* and *R*) polymerized phases of C_{60}. Region *A* is the region of existence of atomic carbon states arising as a result of thermal destruction of the monomeric fcc and polymerized phases of C_{60}. The thick solid line specifies the phase equilibrium boundary between the monomeric fcc phase and the polymerized phases of C_{60}.[14] The two dashed lines correspond: (1) to the thermal stability limits of C_{60} molecules in the monomeric and polymerized phases (upper line), and (2) to the supposed equilibrium line between the *T* and *R* phases. The latter line was plotted rather approximately since more detailed investigations are necessary to refine the *p,T* coordinates of these lines by taking into account hysteresis phenomena.

Path 1 involved loading the sample at room temperature up to 0.5 GPa and heating it up to 873 K at fixed pressure, then increasing pressure up to 2.2 GPa (with the temperature

 ©1998 The American Physical Society

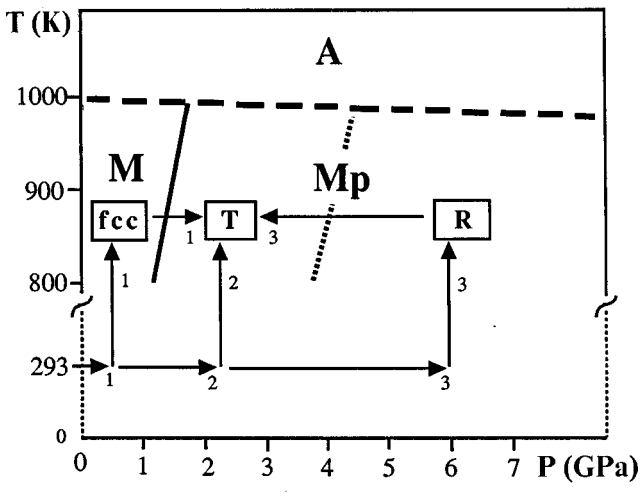

FIG. 1. Fragment of p,T diagram of C_{60} with the three paths (marked by 1, 2, and 3) of phase T synthesis. **A** represents the existence range of atomic carbon. **M** corresponds to the monomeric state. **Mp** corresponds to the range of polymerized phases of C_{60}.

fixed at 873 K), and, finally, holding the sample at 2.2 GPa and 873 K for some exposure time. In this way, phase T is obtained directly from the monomeric fcc phase. On the other hand, path 3 assumed the synthesis of phase T from the R phase. Finally, path 2 assumed the synthesis of the T phase via a low-temperature polymerized phase. Careful identification of the latter is now in progress.

Small-crystalline fullerite C_{60} with impurity content less than 0.1% was taken as a starting material. ''Piston-cylinder'' and ''toroid''-type high-pressure devices were used for HPHTT of fullerite samples. The temperature was directly measured with chromel-alumel thermocouples. The pressure was determined with calibration curves of the pressure-load dependence for the loading and unloading processes at room temperature obtained on the basis of the electroresistivity-pressure dependence of manganin and the electroresistivity anomalies related with pressure-induced phase transition in Bi.[15] Other details of HPHT experiments have been described earlier.[4]

Isothermal exposure times of 1, 10, 100, 1000, 10 000, 20 000 s were used for determination of characteristic relaxation times of the system in the quasiequilibrium state at 2.2 GPa and 873 K for each synthesis path. The exposure times were measured from the moment when the p,T parameters of system reached the values chosen for the T-phase synthesis (2.2 GPa, 873 K). The rate of isothermal loading in the range from 0.5 to 2.2 GPa (path 1) was equal to 0.05 GPa/min and that of isothermal unloading in the range from 6 to 2.2 GPa (path 3) was equal to 0.1 GPa/min. The rate of isobaric heating from 293 to 873 K (path 2) was equal to ~100 K/min.

The products of HPHTT of fullerite were conserved by quenching them down to room temperature under pressure and they were then studied at ambient conditions. Quenching under pressure was also used for conservation of intermediate states arising on different HPHTT stages of experimental paths 1, 2, 3. Care was taken to control the R-phase formation as an intermediate phase of path 3. The completeness of the R-phase formation was assured by isothermal exposure of the samples at 6 GPa and 873 K for as long as 1000 s.

Sample analysis x-ray diffraction and IR and Raman spectroscopy methods were used to characterize the nature of the polymerized states, including the type of structure-forming elements and the way in which they form the three-dimensional structure. The x-ray diffraction (XRD) experiments were carried out by means of an INEL CPS120 position-sensitive detector using the Cu $K\alpha_1$ radiation. Powdered samples were put into Lindemann glass capillaries of 0.5 mm in diameter which were rotated around the θ axis during the experiments. The density of the samples was measured by hydrostatic weighing using ethyl alcohol as liquid.

A DILOR XY Raman spectrometer operating with an Ar^+ laser (514.5 nm) was used to obtain the Raman spectrum. The IR transmission spectra of samples in the KBr matrix were recorded with a Specord M80 spectrometer. Microscopic investigation of samples was made using a scanning-electron microscope DSM 982 Gemini.

The XRD patterns of the carbon states formed at 2.2 GPa, 873 K, with an exposure time of 1 s and different experimental schemes marked as 1,2,3 are shown in Fig. 2. All patterns provide evidence of the presence of the T and R phases in the mixture, but the contents of the two components depend on the paths of HPHTT. Note that the identification of these mixtures only by the XRD analysis alone is a delicate problem because of similarity of the XRD patterns of the $O+T$ and $R+T$ mixtures in the range 8–40° (2Θ). Nevertheless, according to the IR spectral data,[3,6] the presence of the R phase is undoubtedly confirmed. Thus, phase-T content was found to be about 90, 65, and 15 % for the first, second, and third variants of treatment, respectively. The increase in the treatment time led to greater T-phase content in all cases as a result of $R \rightarrow T$ phase conversion. For paths 1 and 2, practically pure T-phase samples were obtained with treatment times of about 1000 and 20 000 s, respectively. For path 3, a phase-T content of about 40% was obtained after a 10 000 s treatment. Analogous evolution pictures were observed in IR and Raman spectra. The x-ray-diffraction pattern of phase T is given in Fig. 2(T). The refined cell parameters of the final sample: $a=9.097(3)$, $c=15.04(2)$ Å, $V=1245(2)$ Å^3, the calculated density is $d_{\mathrm{calc}}=1.92$ g cm^{-3}, the measured density is $d_{\mathrm{meas}}=1.88(1)$ g cm^{-3}, are in agreement with those observed previously for phase T obtained at higher pressures.[2,13] The observed h,k,l values confirm the $h+k+l=2n$ condition of the I-centered crystal lattice, thus giving the packing model of Immm symmetry suggested in Ref. 2. This, however, does not exclude the possibility that, because of the quasisphericity of polymerized C_{60} molecules and the almost tetragonal layer geometry, the reflections with $h+k+l \neq 2n$ are too weak to be observed in the XRD pattern and the body-centering translation is thus not true. In this case an alternative model of $P4_2/mmc$ symmetry is valid. Both models have been compared in our recent computational study of the polymerized C_{60} packing,[12,16] where the preference of the second one was established. The tetragonal character of the layer structures is developed in SEM micrographs. The micrograph of the sample sliver shows the (001) face of phase T [Fig. 3(A)]. The details of the layer sequence parallel to this face can see in Fig. 3(B).

The formation of T polymers of C_{60} reduces the molecular symmetry from the I_h to the D_{2h} point group. Hence, one would expect in the IR spectra of the derivative the appearance of bands originating from the odd modes of the parent

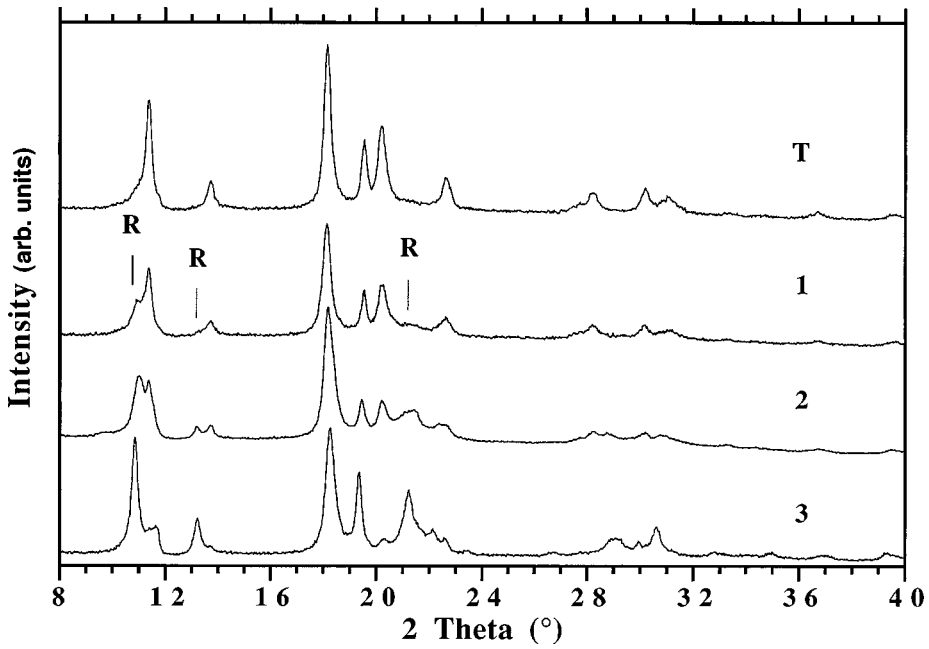

FIG. 2. The XRD patterns (marked as 1,2,3 and containing mixture of *R* and *T* phases) of samples obtained at 2.2 GPa, 873 K, and exposure time 1 s using, respectively, the paths 1,2,3 and the XRD pattern (marked as *T*) of phase *T* obtained by path 1 at exposure time 1000 s.

molecule, and those from the even modes—in Raman scattering. The degeneracy of the *F*, *G*, and *H* modes of icosahedral C_{60} should be removed resulted in the splitting of these modes, respectively, into 3, 4, and 5 components in the Raman spectrum and to triplets in the infrared (A_u modes are inactive due to selection rules). The real IR spectrum (Fig. 4) is rather rich and could hardly be described in terms of a minor distortion of the parent molecule, i.e., the suitable splitting of C_{60}'s active vibrations and the emergence of appropriate multiplets in the established[17] regions of the silent modes. The only spectral interval approximately obeying this rule is around the $F_{1u}(1)$ parent mode and contains a strong band at 522 cm^{-1} (with an unresolved low-frequency shoulder) surrounded by two moderate bands at 510 and 533 cm^{-1}. In the vicinity of the $F_{1u}(2)$ mode a strong band is observed at 557 cm^{-1} indicating the 20 cm^{-1} redshift of the parent mode. Some weak bands detected at 573, 566, 547, and 540 cm^{-1} arose possibly as components of former $F_{1u}(2)$ and $H_u(2)$ modes. There are no intense bands at the wave numbers of the $F_{1u}(3,4)$ modes. Instead, the main features in the region are a moderate band with a maximum at 1261 cm^{-1} and a weak one at 1227 cm^{-1}, both broadened by low-frequency shoulders. They could not be derived from IR-active parent modes and more probably originate from $H_u(5,6)$ or $G_u(5)$ vibrations of the C_{60} molecule observed, respectively, at 1222, 1242, and 1290 cm^{-1}.[17] Maximum spectral intensity is concentrated in the range of 700–800 cm^{-1} where sharp intense bands were observed at 781, 762, 747, and 711 cm^{-1} as well as two broader features at 768 and 733 cm^{-1}. Characteristic for the phase are also the triplet 642/646/654 cm^{-1} and a strong band at 606 cm^{-1}. In the range of 850–960 cm^{-1} where no parent mode is placed, a moderate band emerged at 932 cm^{-1}, along with two weak features at 898 and 882 cm^{-1}. The observed infrared spectrum is much more pronounced than that presented in Ref. 6 (obtained from a ''1:1 mixture of tetragonal and orthorhombic phases'') and differs greatly from it. No traces of oxygen contamination were detected: neither the broad maximum centered at 1100 cm^{-1}, nor the band near 1385 cm^{-1} which characterized a intercalated oxygen.[18] (The latter band could be caused also by an admixture of rhombohedral fragments, but no indication on orthorhombic or rhombohedral impurity was seen in the sample being studied; our results of the spectral comparative study of C_{60}'s *p,T* polymers will be published separately). As the result, much more characteristic bands of the tetragonal phase-forming material were derived.

The Raman spectrum of the sample (Fig. 5) consists of about 35 distinguishable lines. The most intense of them were observed in Ref. 6. The differences of our spectra, obtained from a purer sample, lie in the band's relative intensity and in the structure of multiplets in the high-frequency region. The band at 430 cm^{-1} dominates over the doublet 1447/1464 cm^{-1}; only a very weak line at 710 cm^{-1} and no bands at 1192 and 1459 cm^{-1} were observed, therefore assigned to an impurity. Additional features at 280, 1040, 1208 cm^{-1}, etc., were found to be characteristic for the phase under investigation. The wave numbers of most of the bands could readily be derived from that of Raman-active parent modes of the C_{60} molecule: e.g., the lines at 280, 430, and 1107 cm^{-1} are probably originated from H_g (1, 2, and 5) modes, respectively; the multiplets in the 660–725 and 1550–1575 cm^{-1} regions could arise from $H_g(3)$ and $H_g(8)$ species. The $A_g(1)$ vibration seems to soften from 495 to 486 cm^{-1}; to establish the position of the $A_g(2)$ derivative, one should choose between the two strong lines at 1447 and 1464 cm^{-1}, the remaining one being probably caused by the symmetry-forbidden in the C_{60} $F_{1g}(3)$ mode. Another example of symmetry reduction upon polymerization is the emergence of weak bands at 536, 1208, and 1541 cm^{-1},

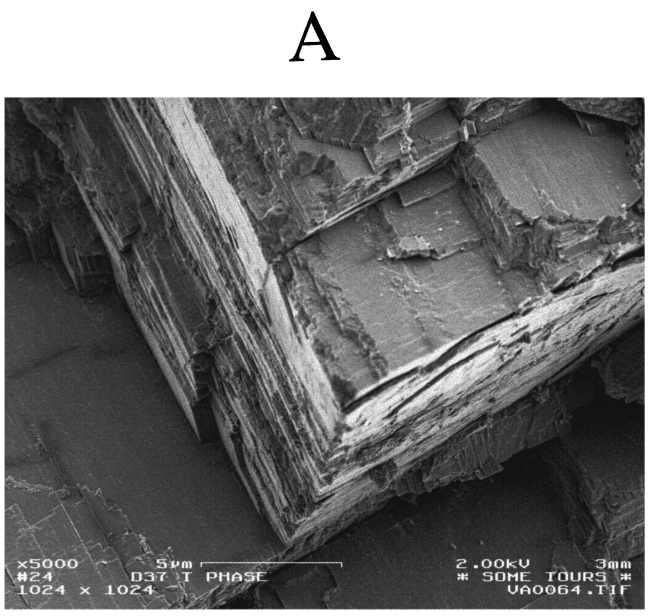

FIG. 3. SEM micrographs of phase *T* sample, (A) (001) face, (B) layers parallel to the (001) face.

probably arising from F_{2g} (1, 3, and 4) modes and very weak features in the 1300–1400 cm^{-1} range originating from G_g(4,5) vibrations. The strong lines at 587 and 949 cm^{-1}, though situated within a 20 cm^{-1} interval from the nearest parent modes, more probably present the even counterparts of the infrared bands at 606 and 932 cm^{-1}. The position of the bands in this region (not their intensity, as was suggested in Ref. 6) were found in our experiments to be quite sensitive to the manner of linkage of the ball indicating that the inter-ball bonds and associated angles participate in these vibrations.

The successful preparation of phase *T* in the pure form showed that this phase has a proper region of existence in the *p,T* diagram of C_{60}. However, the dramatic differences in the rate of *T* phase formation observed for the three paths point

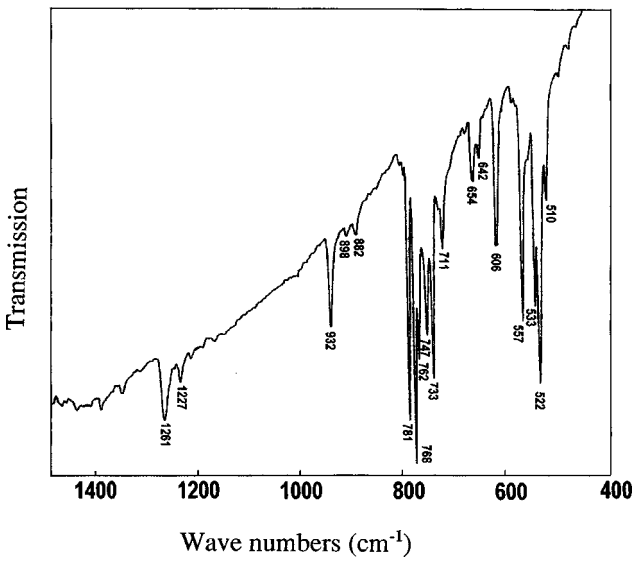

FIG. 4. IR spectrum of phase *T*.

to significant distinction of the mechanisms of phase formation. These mechanisms are determined by the type of that phase which is immediately transformed to the *T* phase.

The present experimental data are in principal agreement with our hypothesis of the possible conversion mechanisms of the monomeric states of C_{60} to the polymerized ones.[12,16] According to this hypothesis, the main prerequisite of the polymerized phase formation is the pressure-induced emergence of orientational-ordered molecular packings that are characterized by close intermolecular contacts of double bonds of adjacent C_{60} molecules in parallel orientation favorable for the $[2+2]$ cycloaddition reaction.[19] Such contacts are not present in the two known fcc and sc molecular structures of C_{60}.[20,21] But, our theoretical calculations showed that each polymerized phase can be provided with a corresponding molecular precursor state occurring as a local potential-energy minimum and having a rough geometrical similarity with the corresponding polymerized phase. The supposed molecular precursor of phase *T* has a quasitetragonal structure $\sim P4_2/m$ (the symbol $\sim$ means some orientational deviations that reduce the space group down to P 1). Thus, the fcc$\rightarrow$*T*-phase reaction can be roughly presented as a two-stage process. The formation of the orientational-ordered molecular precursor of phase *T* is the first stage tak-

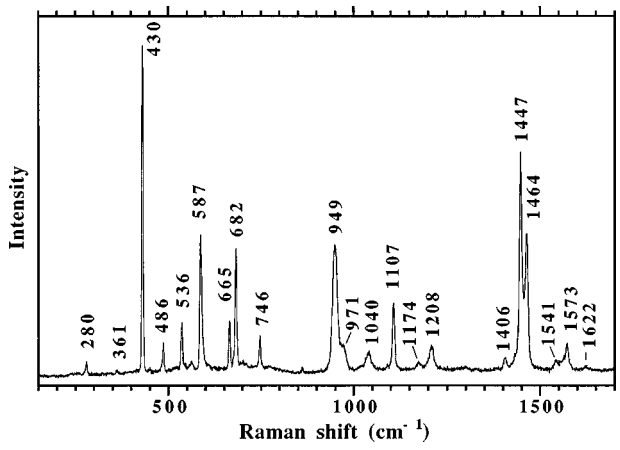

FIG. 5. Raman spectrum of phase *T*.

ing place during the isothermal loading of the fcc phase. The second one is the polymerization of this precursor.

In contrast to this ''direct'' mechanism, yet another conversion stage demanding high activation energies is necessary for the *T*-phase formation from other polymerized phases. For example, the transformation of the rhombohedral lattice into the tetragonal one necessarily demands the breakdown of intermolecular bonds of the *R* phase for the formation of some possible intermediate state—the low-molecular precursor of phase *T*.

In summary, present results indicate that the *T*-polymerized phase is as stable as the *O* and *R* polymerized phases of C_{60}. But it is obvious that an exact determination of the phase equilibrium lines between different polymerized phases will require further study because of the significant hysteresis of these phase transitions.

The present research has been supported by INTAS, Grant No. 93-2133, and by the Russian Fund for Fundamental Research, Grant No. 97-03-33584a.

[1] O. Bethoux, M. Nuñez-Regueiro, L. Marques, J-L. Hodeau, and M. Perroux, in *Proceedings of the Materials Research Society, Boston, 1993*, Abstracts of contributed Papers (Material Research Society, Pittsburgh, 1993), Abstract No. G2.9, p. 202.

[2] M. Nuñez-Regueiro, L. Marques, J-L. Hodeau, O. Berthoux, and M. Perroux, Phys. Rev. Lett. **74**, 278 (1995).

[3] Y. Iwasa, T. Arima, R. M. Fleming, T. Siegrist, O. Zhou, R. C. Haddon, L. J. Rothberg, K. B. Lyons, H. L. Carter, Jr., A. F. Hebard, R. Tycko, G. Dabbagh, J. J. Krajevski, G. A. Thomas, and T. Yagi, Science **264**, 1570 (1994).

[4] V. A. Davydov, L. S. Kashevarova, A. V. Rakhmanina, V. Agafonov, R. Céolin, and H. Szwarc, JETP Lett. **63**, 818 (1996).

[5] L. Marques, J.-L. Hodeau, M. Nuñez-Regueiro, and M. Perroux, Phys. Rev. B **54**, R12 633 (1996).

[6] A. M. Rao, P. C. Eklund, J.-L. Hodeau, L. Marques, and M. Nuñez-Regueiro, Phys. Rev. B **55**, 4766 (1997).

[7] V. A. Davydov, L. S. Kashevarova, A. V. Rakhmanina, A. V. Dzyabchenko, V. Agafonov, P. Dubois, R. Céolin, and H. Szwarc, JETP Lett. **66**, 120 (1997).

[8] L. Marques, J.-L. Hodeau, and M. Nuñez-Regueiro, Mol. Mater. **8**, 49 (1996).

[9] B. Sundqvist, Adv. Phys. (to be published).

[10] B. Sundqvist, Phys. Rev. B **57**, 3164 (1998).

[11] C. H. Xu and G. E. Scuseria, Phys. Rev. B **74**, 274 (1995).

[12] A. V. Dzyabchenko, V. Agafonov, and V. A. Davydov, Kristallografiya (to be published).

[13] V. A. Davydov, L. S. Kashevarova, A. V. Rakhmanina, V. Agafonov, R. Céolin, and H. Szwarc, Carbon **35**, 735 (1997).

[14] I. O. Bashkin, V. I. Rashchupkin, A. F. Gurov, A. P. Moravsky, O. G. Rybchenko, N. P. Kobelev, Ya. M. Soifer, and E. G. Ponyatovsky, J. Phys.: Condens. Matter **6**, 7491 (1994).

[15] G. C. Kennedy and P. N. La Mori, J. Geophys. Res. **67**, 852 (1962).

[16] V. Agafonov, V. A. Davydov, A. V. Dzyabchenko, R. Ceolin, and H. Szwarc, in *Fullerenes. Recent Advances in the Chemistry and Physics of Fullerenes and Related Materials* edited by K. M. Kadish and R. S. Ruoff (The Electrochemical Society, Pennington, NJ, 1997), Vol. 5, p. 373.

[17] M. C. Martin, X. Du, J. Kwon, and L. Mihaly, Phys. Rev. B **50**, 173 (1994).

[18] H. Werner, Th. Schedel-Niedrig, W. Wohlers, D. Herein, B. Herzog, R. Schlogl, M. Keil, A. M. Bradshaw, and J. Kirschner, J. Chem. Soc., Faraday Trans. **90**, 403 (1994).

[19] A. M. Rao, P. Zhou, K.-A. Wang, G. T. Hager, J. M. Holden, Y. Wang, W.-T. Lee, X. X. Bi, P. C. Eklund, D. S. Cornett, M. A. Duncan, and I. J. Amster, Science **259**, 955 (1993).

[20] W. I. F. David, R. M. Ibberson, T. J. S. Dennis, J. P. Hare, and K. Prassides, Europhys. Lett. **18**, 219 (1992).

[21] A. Lundin and B. Sundqvist, Phys. Rev. B **53**, 8329 (1996).